Physics Procedia

Volume 75, 2015, Pages 948–955

20th International Conference on Magnetism

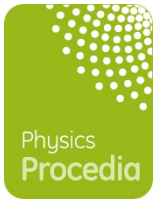

Relativistic effects on electron transport in magnetic alloys

Václav Drchal[1], Josef Kudrnovský[2], and Ilja Turek[3]

[1] Institute of Physics, Academy of Sciences of the Czech Republic, Na Slovance 2, CZ-182 21 Praha 8, Czech Republic
drchal@fzu.cz

[2] Institute of Physics, Academy of Sciences of the Czech Republic, Na Slovance 2, CZ-182 21 Praha 8, Czech Republic
kudrnov@fzu.cz

[3] Institute of Physics of Materials, Academy of Sciences of the Czech Republic, Žižkova 22, CZ-616 62, Brno, Czech Republic
turek@ipm.cz

Abstract

We study the relativistic effects on electron transport in spin-polarized metals and random alloys on ab initio level using the fully relativistic tight-binding linear muffin-tin-orbital (TB-LMTO) method. We employ a Kubo linear-response approach adapted to disordered multisublattice systems in which the chemical disorder is described in terms of the coherent potential approximation (CPA). The CPA vertex corrections are included. We calculate both the Fermi surface and Fermi sea terms of the full conductivity tensor. We find that in cubic ferromagnetic 3d transition metals (Fe, Co, Ni) and their random binary alloys (Ni-Fe, Fe-Si) the Fermi sea term in the anomalous Hall conductivity is small in comparison with the Fermi surface term, however, in more complicated structures, such as hexagonal Co and selected Co-based Heusler alloys, it becomes important. We find an overall good agreement between the theory and experimental data.

Keywords: Relativistic effects, transversal transport, magnetic alloys

1 Introduction

Simultaneous presence of a spontaneous spin polarization and spin-orbit interaction in a solid gives rise to a number of physically interesting and technologically important phenomena, such as magnetocrystalline anisotropy and magnetic dichroism in the X-ray absorption spectra [12]. The anomalous Hall effect [9] (AHE) represents the most famous example of a spin-orbit driven transverse transport phenomenon in itinerant magnets. The AHE is explained in terms of the Berry curvature of occupied Bloch states for perfect crystals [5] and the skew scattering and side-jump mechanisms for systems with impurities [4, 9].

Recently, first-principles studies of specific materials have appeared, devoted to pure ferromagnetic metals and various ordered compounds, including Heusler alloys and partially ordered

Selection and peer-review under responsibility of the Scientific Programme Committee of ICM 2015

doi:10.1016/j.phpro.2015.12.130

alloys. Existing studies are based on the single-particle Green's function (GF) and the coherent potential approximation (CPA) in the framework of the fully relativistic Korringa-Kohn-Rostoker (KKR) or the tight-binding linear muffin-tin orbital (TB-LMTO) methods. Both approaches employ the conductivity tensor formulated in the Kubo linear response theory [7], where the configuration averaging leads to the CPA-vertex corrections [17, 2, 3].

Most of the published results for random alloys rest on the Kubo-Středa formula [13, 4] which provides an expression for the full conductivity tensor at zero temperature solely in terms of quantities at the Fermi energy. However, the calculations could be performed only with the neglect of the term containing the coordinate operator which is not compatible with periodic boundary conditions used in standard bulk techniques. The neglect of the problematic term has been justified by a high degree of symmetry of the crystal lattice (e.g., cubic). The neglected term is equivalent to the so-called Fermi sea contribution which follows from the original Bastin formula for the conductivity tensor [1]. The Fermi sea term does not contain coordinate operator, but it requires energy integration over the occupied part of the valence spectrum. Its direct evaluation for model systems and for realistic band structures of transition metals indicates that, at least in the high-conductivity regime, the Fermi sea term represents a small correction to the dominating Fermi surface term defined only in terms of quantities at the Fermi energy. However, similar studies for qualitatively different systems mentioned above cannot be found in the literature.

The present study is devoted to a formulation of the conductivity tensor from the Bastin formula in the relativistic TB-LMTO method; the focus is on the Fermi sea term and random alloys. The paper is organized as follows. The theory is summarized in Section 2, illustrative examples are shown in Section 3 and the conclusions are presented in Section 4.

2 Theory

2.1 Spin-polarized relativistic electronic structure

We use the relativistic spin-polarized version of the linear muffin-tin orbital (LMTO) method in the atomic sphere approximation (ASA). The Hamiltonian reads

$$H = C + W S^0 \left(1 - \gamma S^0\right)^{-1} W^T, \tag{1}$$

where the C, W (W^T corresponds to $\sqrt{\Delta}$, T denotes transposition), and γ are site-diagonal matrices of potential parameters and the S^0 denotes the matrix of canonical structure constants. In the spin-polarized case the only quantum number is μ which corresponds to the z-component of the total angular momentum J_z. Consequently, the matrices in (1) have two types of indices, namely, $\Lambda = (\kappa\mu)$ connected with the behavior of wave functions at surfaces of the Wigner-Seitz spheres and $\tilde{\Lambda} = (\lambda\mu)$ that reflect the behavior of wave functions in the vicinity of atomic nuclei. For details see [11, 10, 14].

The (physical) Green function $G(z) = (z - H)^{-1}$ is calculated via the auxiliary Green function $g^\alpha(z) = [P^\alpha(z) - S^\alpha]^{-1}$ as $G(z) = \lambda^\alpha(z) + \mu^\alpha(z) g^\alpha(z) \mu^{\alpha T}(z)$, where

$$P^\alpha(z) = \left[W^T (z - C)^{-1} W + \gamma - \alpha\right]^{-1} \tag{2}$$

is the potential function and

$$\lambda^\alpha(z) = \mu^\alpha(z)(\gamma - \alpha) W^{-1}, \quad \mu^\alpha(z) = (W^T)^{-1} \left[1 + (\alpha - \gamma) P^\alpha(z)\right] \tag{3}$$

are site-diagonal quantities, α is a site-diagonal matrix of screening constants. In what follows the auxilliary quantities are in the LMTO representation α, which is not written explicitly.

2.2 Conductivity tensor

Coordinate and velocity operators. The coordinate operator X_μ is represented by a matrix diagonal in the $(\mathbf{R}\tilde{\Lambda})$-index as

$$(X_\mu)_{\mathbf{R}'\tilde{\Lambda}',\mathbf{R}\tilde{\Lambda}} = \delta_{\mathbf{R}'\mathbf{R}}\,\delta_{\tilde{\Lambda}'\tilde{\Lambda}}\,X^\mu_{\mathbf{R}}, \tag{4}$$

where $X^\mu_{\mathbf{R}}$ is the μ-th component of the position vector $\mathbf{R}$. The velocity operator V_μ is then defined as a time derivative of X_μ ($\hbar = 1$):

$$V_\mu = -\mathrm{i}\,[X_\mu, H]\,, \tag{5}$$

where $[A, B] = AB - BA$ denotes a commutator. The simple rule (4) is an approximation of the true continuous coordinate by its step-like integer part constant inside each atomic sphere. This leads to a systematic neglect of intraatomic currents so that the resulting conductivity $\sigma_{\mu\nu}$ describes only the net electron motion between atomic sites [16].

Bastin formula and Kubo-Středa formula. The Bastin formula [1] for the conductivity tensor of a non-interacting electron system reads

$$\sigma_{\mu\nu} = -2\sigma_0 \int \mathrm{d}E f(E) \mathrm{Tr}\left\langle V_\mu G'_+(E) V_\nu [G_+(E) - G_-(E)] - V_\mu [G_+(E) - G_-(E)] V_\nu G'_-(E) \right\rangle . \tag{6}$$

The integral is taken over the whole real energy axis and the function $f(E)$ denotes the Fermi-Dirac distribution function. The prime at the $G_\pm(E)$ denotes the energy derivative. The trace (Tr) in (6) is taken over all orbitals of the system and the symbol $\langle \dots \rangle$ denotes the average over all configurations of the random alloy. The subscripts μ and ν denote Cartesian coordinates ($\mu, \nu \in \{x, y, z\}$), and we abbreviated $G_\pm(E) = G(E \pm \mathrm{i}0)$. The numerical prefactor σ_0 reflects the units employed and the size of the big system; with $\hbar = 1$ assumed here, it is $\sigma_0 = e^2/(4\pi V_0 N)$, where V_0 is the volume of the primitive cell and N is the number of cells in a big finite crystal with periodic boundary conditions. By employing the auxiliary quantities we get

$$\sigma_{\mu\nu} = -2\sigma_0 \int \mathrm{d}E f(E) \mathrm{Tr}\langle v_\mu g'_+(E) v_\nu [g_+(E) - g_-(E)] - v_\mu [g_+(E) - g_-(E)] v_\nu g'_-(E)\rangle. \tag{7}$$

This form is identical with the original one, but the Eq. (7) has clear advantages in the configuration averaging for two reasons. First, the full resolvents $G_\pm(E)$ are replaced by the auxiliary GFs for which the CPA-average $\bar{g}(z)$ can be directly evaluated. Second, the random velocities V_μ are replaced by the non-random effective velocities $v_\mu = -\mathrm{i}\,[X_\mu, S]$ so that the configuration average of the whole conductivity tensor can be performed by following the standard formulation of the CPA-vertex corrections [17, 3]. The expression (7) can be further modified (see Refs. [4, 15]) to the form $\sigma_{\mu\nu} = \sigma^{(1)}_{\mu\nu} + \sigma^{(2)}_{\mu\nu}$, where the first term (called the Fermi surface term) is

$$\sigma^{(1)}_{\mu\nu} = \sigma_0 \int \mathrm{d}E f'(E) \mathrm{Tr}\langle v_\mu g_+(E) v_\nu [g_+(E) - g_-(E)] - v_\mu [g_+(E) - g_-(E)] v_\nu g_-(E)\rangle, \tag{8}$$

and the second term (called the Fermi sea term) is

$$\begin{aligned} \sigma^{(2)}_{\mu\nu} \;=\; \sigma_0 \int \mathrm{d}E f(E) \mathrm{Tr}\left\langle v_\mu g_+(E) v_\nu g'_+(E) - v_\mu g'_+(E) v_\nu g_+(E) \right. \\ \left. - v_\mu g_-(E) v_\nu g'_-(E) + v_\mu g'_-(E) v_\nu g_-(E) \right\rangle . \end{aligned} \tag{9}$$

The zero-temperature case of the Fermi sea term (9) can be recast into a contour integral in the complex energy plane:

$$\sigma_{\mu\nu}^{(2)} = \sigma_0 \int_C \mathrm{d}z \mathrm{Tr}\, \langle v_\mu g'(z) v_\nu g(z) - v_\mu g(z) v_\nu g'(z) \rangle \,, \tag{10}$$

where the integration path C starts and ends at E_F, it is oriented counterclockwise and it encompasses the whole occupied part of the alloy valence spectrum. Note that the Fermi sea term is antisymmetric, $\sigma_{\mu\nu}^{(2)} = -\sigma_{\nu\mu}^{(2)}$, so that it contributes only to the anomalous Hall conductivity (AHC) while the longitudinal conductivities are given solely by the Fermi surface term.

The Fermi sea term, obtained from the Kubo-Bastin formulation can be transformed into the corresponding term of the Kubo-Středa formula, namely, $\sigma_{\mu\nu}^{(2)} = \mathrm{i}\sigma_0 \mathrm{Tr}\langle (X_\mu v_\nu - X_\nu v_\mu)[g_+(E_\mathrm{F}) - g_-(E_\mathrm{F})]\rangle$. This transformation is formally exact, but the transformed result contains the coordinate operator that is unbounded and incompatible with the periodic boundary conditions used in the numerical implementation.

For simple systems with inversion symmetry (cubic, hexagonal close-packed), the lattice summations can be rearranged in such a way that the resulting $\sigma_{\mu\nu}^{(2)}$ vanishes identically, in contrast to the results of Eq. (10). Since the Kubo-Bastin approach does not involve the problematic coordinate operator and since the direct evaluation of $\sigma_{\mu\nu}^{(2)}$ yields non-zero values even for the simplest systems, the formula (10) represents a correct version of the Fermi sea term within the TB-LMTO formalism.

The configurational average of the integrand in (10) contains only the coherent part

$$\mathrm{Tr}\, \langle v_\mu g'(z) v_\nu g(z) - v_\mu g(z) v_\nu g'(z) \rangle = \mathrm{Tr}\, \{ v_\mu \bar{g}'(z) v_\nu \bar{g}(z) - v_\mu \bar{g}(z) v_\nu \bar{g}'(z) \} \,, \tag{11}$$

because the vertex corrections vanish (for details of derivation see [15]). On the other hand, the energy derivative $\bar{g}'(z)$ in (11) is expressed as $\bar{g}'(z) = -\bar{g}(z)\mathcal{P}'(z)\bar{g}(z)$, where $\mathcal{P}(z)$ is the coherent potential function. It turns out, however, that $\mathcal{P}'(z)$ can be calculated using the procedure which is basically the same as the evaluation of vertex corrections (see Appendix A in [15]).

Internal consistency of the theory. The TB-LMTO method is formulated in a general LMTO representation specified by a set of site-diagonal screening constants [14]. Here we show that the conductivity is independent of screening constants. Let us write the conductivity tensor as $\sigma_{\mu\nu} = \sigma_{\mu\nu,\mathrm{coh}}^{(1)} + \sigma_{\mu\nu,\mathrm{VC}}^{(1)} + \sigma_{\mu\nu}^{(2)}$, where the first and the second term denote, respectively, the coherent and the incoherent (vertex) part of the Fermi surface term (8). It can be shown (see Appendix B in [15]) that the following quantities are invariant: (i) the total tensor $\sigma_{\mu\nu}$, (ii) the incoherent Fermi surface term $\sigma_{\mu\nu,\mathrm{VC}}^{(1)}$, and (iii) the sum of the coherent Fermi surface term and of the Fermi sea term, $\sigma_{\mu\nu,\mathrm{coh}}^{(1)} + \sigma_{\mu\nu}^{(2)}$. Since the Fermi sea term is antisymmetric, the last property means that the symmetric part of the coherent Fermi surface term, $[\sigma_{\mu\nu,\mathrm{coh}}^{(1)} + \sigma_{\nu\mu,\mathrm{coh}}^{(1)}]/2$, is also invariant.

These properties prove the importance of the Fermi sea term for the complete TB-LMTO-CPA theory of the AHE. The LMTO transformation properties together with the purely coherent nature of the Fermi sea term (9) and with its regular behavior in diluted alloys are relevant for a classification of the intrinsic and extrinsic contributions to the AHE. Within the present TB-LMTO formalism, the intrinsic AHC has to be identified with the antisymmetric part of the sum of the coherent Fermi surface term and of the Fermi sea term $[\sigma_{\mu\nu,\mathrm{coh}}^{(1)} + \sigma_{\mu\nu}^{(2)}]$, whereas the

extrinsic AHC is given by the antisymmetric part of the incoherent Fermi surface term $\sigma^{(1)}_{\mu\nu,\mathrm{VC}}$. This seems to be a natural generalization of the classification introduced recently in the KKR method using the Kubo-Středa formula [6].

3 Applications

3.1 Numerical implementation

The LMTO representation giving the most localized real-space structure constants for the valence basis of *s*-, *p*-, and *d*-type orbitals was used. For the parametrization of the local density functional the Vosko-Wilk-Nusair exchange-correlation potential was used. For calculations of the Fermi surface term, a small imaginary part of $\pm 10^{-5}$ Ry has been added to the Fermi energy while in the evaluation of the Fermi sea term (10), the integration has been performed along a circular contour of a diameter 1.5 Ry. The contour integral was approximated by a sum over 20 – 40 complex nodes on the upper semicircle; the nodes were located in an asymmetric way which results in a denser mesh near the Fermi energy. The number of $\mathbf{k}$ vectors sampling the Brillouin zone depends on the distance between the particular complex node and the Fermi energy; for the node closest to the Fermi energy, total numbers of $\sim 10^8$ $\mathbf{k}$ vectors have been used. Convergence tests with respect to the numbers of energy nodes and of $\mathbf{k}$ vectors have been performed for each system, which guarantee reliability of the results.

3.2 3d magnetic metals and their alloys

The calculated AHCs for pure Fe, Co and Ni, compared with other theoretical results and with measured values, are shown in Table 1. The magnetization vector was taken along the [001] direction for cubic metals while for hcp Co the magnetization was considered along the hexagonal *c* axis (easy axis) and also lying in the *ab* plane. Note that the theoretical approaches based on the Berry curvature include both the Fermi surface and the Fermi sea terms, whereas the published KKR results contain only the surface term. The total AHCs calculated in present work are in reasonable agreement with other theoretical results. The AHC of bcc Fe is in a fair agreement with experiment. Bigger discrepancies are found for Co and for Ni. The latter disagreement is ascribed to electron correlations, not treated properly within the local spin-density approximation (LSDA). The calculated Fermi sea term is essentially negligible in fcc Co and Ni, and it represents a weak effect as compared to the Fermi surface term in bcc Fe. A completely different picture is obtained for hcp Co, where the Fermi sea term amounts nearly to 40% of the total AHC, irrespective of the orientation of the magnetization, i.e., the relative anisotropy of the Fermi sea term is similar to that of the Fermi surface term. The inclusion of the Fermi sea term brings the present TB-LMTO results in a better agreement with those of the Berry-curvature approach and with experiment. Our calculations show that the previous statements about the dominating Fermi surface term in metallic systems with high longitudinal conductivities are not generally valid.

An example of the calculated AHC in a concentrated random alloy is presented in Table 2 for the fcc $\mathrm{Ni}_{1-c}\mathrm{Fe}_c$ system. The Fermi sea term represents a very small correction to the dominating Fermi surface term, as expected from the similar situation in pure elements Fe and Ni.

Another study concerns the high-conductivity regime of diluted bcc $\mathrm{Fe}_{1-c}\mathrm{Si}_c$ alloys, being motivated by recent experiments for systems with Si impurity concentrations $c \leq 0.01$. The calculated AHCs are given in Table 3 together with the measured data; the total theoretical

	bcc Fe	hcp Co (c)	hcp Co (ab)	fcc Co	fcc Ni
Experiment	1032[a]	~ 813[b]	~ 150[b]	727[c]	-1100[d]
Berry curvature	751[e]	481[b]	116[b]	249[b]	-2203[f]
KKR method	685[g]	325[g]		213[g]	-2062[g]
This work total	796	471	169	359	-2432
This work Fermi sea	179	181	66	-5	-17

[a]P.N. Dheer, Phys. Rev. 156:637 (1967); [b]E. Roman et al., Phys. Rev. Lett. 103:097203 (2009);
[c]D. Hou et al., J. Phys.: Condens. Matter 24:482001 (2012); [d]L. Ye et al., Phys. Rev. B 85:220403 (2012);
[e]Y. Yao et al., Phys. Rev. Lett. 92:207208 (2004); [f]X. Wang et al., Phys. Rev. B 76:195109 (2007);
[g]D. Ködderitzsch et al., New J. Phys. 15:053009 (2013).

Table 1: The experimental and calculated values of the AHC (in S/cm) for ferromagnetic $3d$ transition metals. Two columns for hcp Co refer to the magnetization direction along the c axis (c) and in the ab plane (ab).

values were decomposed into the intrinsic and extrinsic parts as defined in Section 2.2. One can see a sign change of the AHC in a semiquantitative agreement with experiment; this effect can be obviously ascribed to a strong variation of the extrinsic part, which diverges for $c \to 0$ due to the skew scattering mechanism, whereas the intrinsic part approaches smoothly the AHC of pure Fe. Note that the Fermi sea term, which enters the intrinsic part, is independent of Si concentration and it becomes non-negligible for compositions with a very small total AHC. This system is an example of a ferromagnetic metal containing very light impurities with a negligible strength of the spin-orbit interaction and a weak exchange splitting. The diverging AHC and the change of its sign in the diluted Fe-Si alloy prove clearly that such light non-magnetic impurities in a feromagnetic host with spin-orbit coupling can lead to pronounced skew-scattering effects in the transverse transport.

c	0.0	0.05	0.10	0.15	0.20	0.25	0.30	0.40	0.50	0.60
total	-2432	-981	52	410	516	492	463	418	457	544
Fermi sea	-17	-5	4	11	18	25	32	48	66	90

Table 2: The calculated values of the total AHC σ_{xy} and of the Fermi sea contribution (in S/cm) for disordered fcc $Ni_{1-c}Fe_c$ alloys as functions of Fe concentration c.

c	0.0	0.003	0.005	0.010	0.020
experiment[a]		-1000		700	
total	796		-714	141	557
Fermi sea	179		177	174	165
intrinsic	796		701	708	687
extrinsic			-1415	-567	-130

[a]Y. Shiomi et al., Phys. Rev. B 79:100404 (2009).

Table 3: The values of the AHC σ_{xy} in diluted bcc $Fe_{1-c}Si_c$ alloys as functions of Si concentration c. The experimental values and the calculated values of the total AHC, Fermi sea contribution, intrinsic and extrinsic parts are given (in units S/cm).

3.3 Co-based Heusler alloys

The AHE has also been studied intensively in Co-based Heusler alloys Co_2CrAl and Co_2MnAl, both experimentally and theoretically. There is a generally accepted view that the structure and chemical composition of measured samples differ from those of ideal $L2_1$ compounds. These imperfections are responsible for a discrepancy between the calculated and measured magnetic moments, strong especially for the Co_2CrAl system, as well as for relatively high longitudinal resistivities of both systems [8]. Table 4 displays the total AHCs for both ideal compounds and for three disordered systems of compositions $(Co_{1-c}Cr_c)_2(Cr_{1-2c}Co_{2c})Al$ and $Co_2(X_{1-c}Al_c)(Al_{1-c}X_c)$ with $c = 0.25$ and X = Cr, Mn. The main conclusions that the strong reduction of the AHC of the ideal compounds by the antisite disorder and the small extrinsic (vertex corrections) part of the AHC [8] are robust with respect to inclusion of the Fermi sea term. Relative values of the latter term lie between 20 and 40 % of the total AHC; the only exception is the Co_2CrAl alloy with 25% of Cr-Al swap, where the Fermi sea term is essentially negligible.

A	B	C	D	total	Fermi sea
Co	Cr	Co	Al	400	−107
$Co_{0.75}Cr_{0.25}$	$Cr_{0.5}Co_{0.5}$	$Co_{0.75}Cr_{0.25}$	Al	144	39
Co	$Cr_{0.75}Al_{0.25}$	Co	$Al_{0.75}Cr_{0.25}$	129	4
Co	Mn	Co	Al	1787	728
Co	$Mn_{0.75}Al_{0.25}$	Co	$Al_{0.75}Mn_{0.25}$	452	90

Table 4: The calculated values of the total AHC and of the Fermi sea contribution for selected ordered and disordered Co-based Heusler alloys (in S/cm). First four columns (denoted as A, B, C, and D) show the occupation of four sublattices of the Heusler alloy.

4 Conclusions

We have extended our recent transport theory in the relativistic TB-LMTO method by a formulation and numerical implementation of the Fermi sea term, which follows from the Bastin formula for the conductivity tensor and which contributes to the AHE. In the case of random alloys treated in the CPA, the configuration averaging of this term revealed its purely coherent nature, with effective vertex corrections originating in the energy dependence of the average single-particle propagators. The behavior of the Fermi sea term in the dilute limit of a random alloy is in general regular, in contrast to the often diverging Fermi surface term. We have further examined the transformation properties of the conductivity tensor with respect to the choice of the LMTO representation. This analysis proved the importance of the Fermi sea term for the representation invariance of the total AHCs and of their intrinsic part.

Calculations performed with the best screened LMTO representation for several qualitatively different systems confirmed in most cases an expected fact, namely, significantly smaller values of the Fermi sea term as compared to the Fermi surface term. Notable exceptions refer to uniaxial systems (hexagonal cobalt) and to multisublattice multicomponent systems (Heusler alloys). However, even in these cases, the inclusion of the Fermi sea term did not change qualitatively the most important features of the AHE, such as its anisotropy or sensitivity to antisite defects.

Acknowledgments

The authors thank Czech Science Foundation (Project 15-13436S) for financial support.

References

[1] A. Bastin, C. Lewiner, O. Betbeder-Matibet, and P. Nozieres. Quantum oscillations of the Hall effect of a fermion gas with random impurity scattering. *J. Phys. Chem. Solids*, 32:1811, 1971.

[2] W. H. Butler. Theory of electronic transport in random alloys: Korringa-Kohn-Rostoker coherent-potential approximation. *Phys. Rev. B*, 31:3260, 1985.

[3] K. Carva, I. Turek, J. Kudrnovský, and O. Bengone. Disordered magnetic multilayers: electron transport within the coherent potential approximation. *Phys. Rev. B*, 73:144421, 2006.

[4] A. Crépieux and P. Bruno. Theory of anomalous Hall effect from the Kubo formula and the Dirac equation. *Phys. Rev. B*, 64:014416, 2001.

[5] T. Jungwirth, Q. Niu, and A. H. MacDonald. Anomalous Hall effect in ferromagnetic semiconductors. *Phys. Rev. Lett.*, 88:207208, 2002.

[6] D. Ködderitzsch, K. Chadova, J. Minár, and H. Ebert. Impact of finite temperatures and correlations on the anomalous hall conductivity from ab initio theory. *New J. Phys.*, 15:053009, 2013.

[7] R. Kubo. Statistical-mechanical theory of irreversible processes I. *J. Phys. Soc. Jpn.*, 12:570, 1957.

[8] J. Kudrnovský, V. Drchal, and I. Turek. Anomalous Hall effect in stoichiometric Heusler alloys with native disorder: a first-principles study. *Phys. Rev. B*, 88:014422, 2013.

[9] N. Nagaosa, J. Sinova, S. Onoda, A. H. MacDonald, and N. P. Ong. Anomalous Hall effect. *Rev. Mod. Phys.*, 82:1539, 2010.

[10] A. B. Shick, V. Drchal, J. Kudrnovský, and P. Weinberger. Electronic structure and magnetic properties of random alloys: fully relativistic spin-polarized linear muffin-tin orbital method. *Phys. Rev. B*, 54:1610–1621, 1996.

[11] I. V. Solovyev, A. I. Lichtenstein, V. A. Gubanov, V. P. Antropov, and O. K. Andersen. Spin-polarized relativistic linear-muffin-tin-orbital method: Volume-dependent electronic structure and magnetic moment of plutonium. *Phys. Rev. B*, 43:14414, 1991.

[12] P. Strange. *Relativistic Quantum Mechanics*. Cambridge University Press, Cambridge, England, 1999.

[13] P. Středa. Theory of quantised Hall conductivity in two dimensions. *J. Phys. C: Solid State Phys.*, 15:L717, 1982.

[14] I. Turek, V. Drchal, J. Kudrnovský, M. Šob, and P. Weinberger. *Electronic Structure of Disordered Alloys, Surfaces and Interfaces*. Kluwer, Boston, 1997.

[15] I. Turek, J. Kudrnovský, and V. Drchal. Fermi sea term in the relativistic linear muffin-tin-orbital transport theory for random alloys. *Phys. Rev. B*, 89:064405, 2014.

[16] I. Turek, J. Kudrnovský, V. Drchal, L. Szunyogh, and P. Weinberger. Interatomic electron transport by semiempirical and ab initio tight-binding approaches. *Phys. Rev. B*, 65:125101, 2002.

[17] B. Velický. Theory of electronic transport in disordered binary alloys: coherent-potential approximation. *Phys. Rev.*, 184:614, 1969.